Available online at www.sciencedirect.com
ScienceDirect
Journal of Sound and Vibration 323 (2009) 112–129
JOURNAL OF SOUND AND VIBRATION
www.elsevier.com/locate/jsvi

Real time aircraft fly-over noise discrimination

M. Genescà*, J. Romeu, T. Pàmies, A. Sánchez

Acoustic and Mechanical Engineering Laboratory (LEAM), Technical University of Catalonia C/ Colom 11, 08222 Terrassa, Spain

Received 13 September 2007; received in revised form 18 November 2008; accepted 23 December 2008
Handling Editor: P. Joseph
Available online 20 February 2009

Abstract

A method for measuring aircraft noise time history with automatic elimination of simultaneous urban noise is presented in this paper. A 3 m-long 12-microphone sparse array has been proven to give good performance in a wide range of urban placements. Nowadays, urban placements have to be avoided because their background noise has a great influence on the measurements made by sound level meters or single microphones. Because of the small device size and low number of microphones (that make it so easy to set up), the resolution of the device is not high enough to provide a clean aircraft noise time history by only applying frequency domain beamforming to the spatial cross-correlations of the microphones' signals. Therefore, a new step to the processing algorithm has been added to eliminate this handicap.

1. Introduction

Airport noise monitoring is, in most cases, performed by placing soundmeters near the airport. These sound level meters transmit noise level data in real time. However, not all sound level meters placements are suitable. Only those with low background noise level should be attempted in order to obtain an aircraft noise history as pure as possible. This placement limitation becomes a disadvantage when interest is focused on measuring aircraft emission levels in an urban area [1], since urban centers have, in general, high background noise levels. If urban center locations are attempted, further processing is needed to distinguish between peaks caused by aircraft flying over and peaks caused by traffic noise. In most cases, use has to be made of the airport's schedule of departures and arrivals in order to track down peaks caused by aircraft.

The main drawbacks to this classical airport noise monitoring method are:

- Other noise events are mistaken for an airplane. A car passing by in a quiet area, for instance, may have an acoustic time history similar to that of an airplane and, thus, can be mistaken. In order not to make such a mistake, acoustic data should be correlated with the departure/arrivals schedule of the airport.
- Background noise added to the airplane noise. Other noise events can occur simultaneously to the airplane flying over, for example traffic noise. In that case it cannot be determined which part of the overall level is caused by the airplane and which part is caused by traffic noise. This can be an important point in some

*Corresponding author. Tel.: +34 937398717; fax: +34 937398145.
E-mail address: meritxell.genesca@upc.edu (M. Genescà).

0022-460X/$ - see front matter © 2009 Elsevier Ltd. All rights reserved.
doi:10.1016/j.jsv.2008.12.030

airports where companies and pilots are subjected to economic fines if noise levels thresholds are exceeded at some control points.

- Floor reflections added to the direct noise. Although microphones are placed as far from the floor as possible in order to avoid reflections, noise levels will always be increased by reflections to a greater or lesser extent, depending on the soil characteristics.

Several attempts have been made in order to make an automatic decision whether a peak is caused by an airplane or not. Some of these methods are based on the fulfillment of two conditions. The first is the temporal correlation between the noise levels time history and the flight paths, and the second is when a trigger noise level is exceeded, which is supposed to be reached only when the peak is caused by an airplane [2–4]. In some studies instead of a threshold level, a transition region is taken in such a way that every level inside this region has an associated probability to the peak generated by an airplane, so the peak is assumed to be partially generated by the airplane in a percentage proportional to this probability [5].

When there is no data available about the flight path (for security purposes it is often unavailable), another set of methods exists. Complex systems based on the measurement of sound intensity instead of sound pressure exist. The goal is to use microphones in pairs with different spatial directions to obtain a three dimensional intensity vector, which ensures that when the airplane is the main source, the vector points towards it, detecting the airplane as it passes by. This fact can be used as a trigger to start measuring noise levels and assign them to the airplane. One of the problems of this system is that the intensity vector points towards the main source, and thus if an acoustic event as loud as an airplane fly-over occurs (such as a car passing by) the vector points towards an intermediate position [6].

Other techniques aimed at determining if an acoustic event is caused by an airplane or not are based on neural network identification. These techniques focuses the attention on the signal characteristics such as frequency content, signal temporal history, or signal frequency content evolution so as to train a neural network in airplane recognition [7–11].

All these techniques listed above are capable of determining the time period when an airplane is passing by, but they still have the problem of measuring the airplane noise mixed with background noise, and also with floor reflections.

It seems that background noise and airplane noise could be separated using a model based on the human auditory brain system, which is based on the interplay of autocorrelators and an interaural cross-correlator acting on the pressure signals arriving at the ear entrances, and taking into account the specialization of left and right human cerebral hemispheres [12]. However, it has been demonstrated that other techniques that are based on directional measurements are clearly capable of distinguishing airplane noise from other noise. The aim here is to design a system capable of measuring noise coming from certain directions in space. Such a goal can be achieved by using an array of microphones instead of a single microphone or sound level meter [13–15]. The theoretical base is that the sound will not reach all the microphones at the same time instant but rather a delay will appear between the signals provided by the microphones. Such a delay is related to the arrival direction of the sound sources.

Microphone arrays have been used before in a great variety of fields such as transportation in order to detect acoustic sources on vehicles [16–27] and in aeronautics where it has been applied mainly with the aim of detecting airframe noise in the airplane fuselage [28–34].

With the aim of measuring aircraft noise, some devices with a low number of microphones have been tested [35,36] They are limited in spatial resolution when finding the direction of the propagation of the noise; therefore they are only able to determine whether the noise came from above or below. Thus, when such a device is placed in a place high enough to ensure that all traffic noise came from below, it only acts as a trigger to start recording when noise from above is detected. This means that for these devices, airplane noise record is mixed with background noise as well as with floor reflections.

In order to avoid the presence of background noise in the airplane noise recording, use should be made of large arrays [37–41] which give higher spatial resolution and are capable of separating noise coming from different directions.

2. Aircraft noise

In order to define the frequency range of interest, several aircraft noise measurements were performed. They took place near to the Barcelona Airport, and a total of 25 different kinds of aircraft were measured while taking off. The measurements suggest that the main noise contribution is within 125–2000 Hz octave bands, which is the same result found by other authors [41]. Low frequency contribution becomes more important as the distance between the source and the airplane increases because of atmospheric attenuation [42], which is larger for high frequencies. In the same way, although guidelines for aircraft certification require measuring an airplane's spectra up to 10 kHz, such a wide range is not applied here due to the effect of atmospheric attenuation on high frequencies. The objective of this paper is to apply microphone array based techniques to measure airplane noise, making a distinction between airplane noise and traffic noise generated simultaneously.

3. Theoretical background

A microphone array consists of a grid of microphones sampling the sound field at discrete spatial positions. The number of dimensions in the grid restrict the number of available coordinates of the sound source position. For instance, a linear microphone array placed in the vertical axis will only make it possible to determine the vertical angle where the sound source is found, not the horizontal angle nor the range needed to exactly place the source. This fact only allows to state that the source is placed on a conic surface around the microphone antenna axis.

In this paper the goal is not to place the source but rather to separate airplane noise from traffic noise. Making the assumption that the antenna is set up on a roof or a terrace, then the problem becomes to separate between noise coming from above (airplane noise) and noise coming from below (urban noise). Therefore, a linear array will be enough since only one of the source position coordinates (vertical angle) is of interest. Different microphone configurations can be evaluated for the linear array:

- a regular grid of periodically spaced sensors (full array),
- a regular grid of periodically spaced sensors with some vacant positions (sparse array), and
- an irregular grid of sensors (irregular array).

Regular arrays are desirable because although spatial aliasing is most common than in the case of irregular arrays, they permit the use of fast algorithms such as FFT to analyze the data. Full array and sparse array characteristics will be discussed later (Section 3.1).

The basic principle for sound source location with a linear array is that given an arbitrary airplane wave which propagates to the antenna with an angle α (respect the x-axis), and with the sound speed c (Fig. 1), the propagation speed of the wave fronts in the y-direction (c') can be obtained from:

$$c' = c/\sin\alpha \tag{1}$$

Thus, if several microphones are placed and aligned in the y-direction, the acoustic pressure in each of them will be given by

$$p(d_i, t) = p(t - d_i/c') \tag{2}$$

where d_i is the distance between the microphone i and the reference microphone, i.e the highest microphone in the array ($d_0 = 0$). $p(t)$ is the acoustic pressure in the reference microphone.

It can be seen from Eqs. (1) and (2), that the delay between a pair of sensors is a function of the sound wave's angle of incidence α. This is the theoretical principle that allows a multiple microphone system to infer the direction of propagation of a sound wave impinging on it. But doing this is not so easy when multiple waves are impinging on the array of microphones; in this case a more complex process has to be performed in order to obtain information about the propagation direction of each wave. Rearranging Eq. (1) in terms of

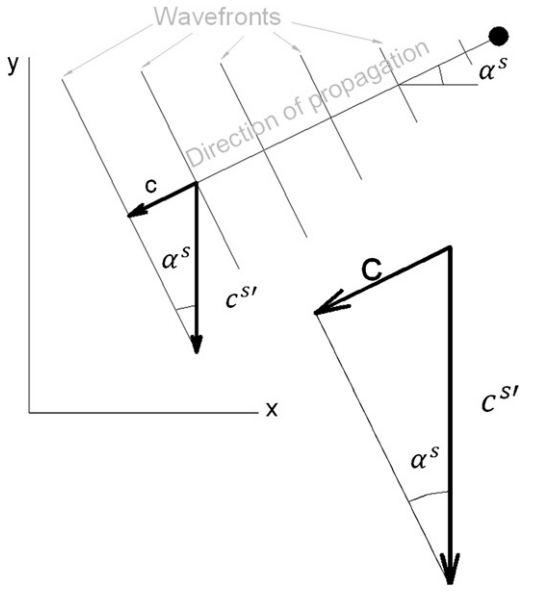

Fig. 1. Wave fronts impinging on the array with an angle α relative to the normal of the antenna axis. The linear microphone array is assumed to be placed in the *y*-direction.

frequency (f) and spatial frequency (v'), results in

$$v' = (f/c)\sin\,\alpha \tag{3}$$

This means that, for every incident wave, the relation between its frequency and the array's estimation of its spatial frequency depends on the propagation direction of the wave. Working with Eq. (3) instead of Eq. (1) allows for all the processing to be done in the frequency domain which, in many cases, has superior characteristics to its time domain counterpart.

3.1. Power spectrum estimation from a double Fourier transform

To determine the incidence angle of an airplane sound waves generated by a source using Eq. (3), a double Fourier transform is required in order to make the conversion from space-time domain ($p(d_i,\ t)$) to spatial frequency–temporal frequency domain ($P(v',\ f)$). This is in the case of having a full array. However, the same calculation scheme can be applied to the cross-correlation function (R) between each microphone pair ij ($R(\Delta d_{ij},\ t)$ with $\Delta d_{ij} = d_i - d_j$) instead of to the microphone signals itself ($p(d_i,\ t)$). In that way, periodicity (in order to apply FFT algorithms) has to be found in Δd_{ij}, not in d_i. This means that microphones should be placed in a way that, given a fundamental distance d, a pair of microphones exists for every $\Delta d_{ij} = nd$ with $n = 1,2,3,\ldots,K$. The aim is to place the microphones in order to maximize K. This configuration is what is called a sparse array. The benefit of using a sparse array is that a larger array can be achieved with the same number of microphones. This results in a resolution increment since resolution is proportional to the antenna length (see Section 4). The calculation sequence for a sparse array is expressed below:

The mth term of the discrete Fourier transform of the sound pressure measured in one microphone with a block size N is calculated by

$$P_m = \frac{1}{N}\sum_{n=0}^{N-1} p_n\, \mathrm{e}^{-\mathrm{j}2\pi nm/N} \tag{4}$$

Then, the mth term of the cross-spectrum between two microphones is calculated by

$$G_m(\Delta d_{ij}) = P_m^*(d_i)P_m(d_j) \tag{5}$$

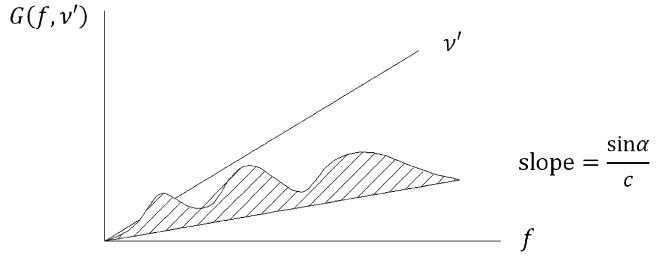

Fig. 2. Isolated signal autospectrum of a source that impinges on the array with an incidence angle α. It appears projected on a straight line in the plane $f-v'$ whose slope is related to the incidence angle. The projection line is different for every source and it leads to the decomposition of the sound field as a function of the incidence angle.

The spatial transform is calculated as follows, given that $\Delta d_{ij} = nd$:

$$G(f, v') = \frac{1}{X}\sum_{n=K}^{K} G(f, nd)\mathrm{e}^{\mathrm{j}2\pi nd v'} d \tag{6}$$

Where X is the synthetic antenna length.

X is not the physical length of the antenna. The physical antenna length is given by $L = Kd$, but since

$$G(f, \Delta d) = G^*(f, -\Delta d) \tag{7}$$

negative values of Δd can be virtually sampled, so the synthetic aperture is

$$X = (2K + 1)d \tag{8}$$

Under this circumstance the discrete values of v' are given by

$$v' = m\left(\frac{1}{2K+1}\right) \tag{9}$$

Thus, the mth term of the spatial frequency–temporal frequency spectrum will be given by

$$G_m = \frac{1}{2K+1}\sum_{n=K}^{K} G(f, nd)\mathrm{e}^{\mathrm{j}2\pi nm/2k+1}$$

The plot of the double frequency spectrum as a function of f and v' results in a surface on which the autospectrum of the signal coming from a given α can be read, since it is the interference between the surface and the perpendicular airplane to f–v'directed by Eq. (3). Fixing a direction α and finding the autospectrum in this direction is what is done to focus the array. Fig. 2 graphically expresses this.

4. Array design

As an easy to use device is wanted, antenna length is limited to 3 m. Fundamental spatial sampling d is limited by the upper boundary of the frequency range of interest which is 2828 Hz (see Section 2), and in order to avoid spatial aliasing the following condition should be fulfilled:

$$d \leqslant \lambda_{\min}/2 \tag{10}$$

Therefore the fundamental sampling distance should be

$$d \leqslant 0.06\,\mathrm{m}$$

As a consequence, for an antenna length of 3 m, if a full array is used, 51 microphones are needed. However, with a sparse array configuration, that length can be covered with only 12 microphones if the following distribution is used [43]:

$$[0\ \ 1\ \ 2\ \ 3\ \ 23\ \ 28\ \ 32\ \ 36\ \ 40\ \ 44\ \ 47\ \ 50]d$$

Table 1
Resolution vs. incidence angle for waves of 88 Hz.

Incidence angle (°)	0	10/−10	20/−20	30/−30	40/−40	50/−50	60/−60	70/−70	80/−80
Resolution (°)	36.9	37.4	39.2	42.6	48.1	57.3	73.7	107.8	212.3

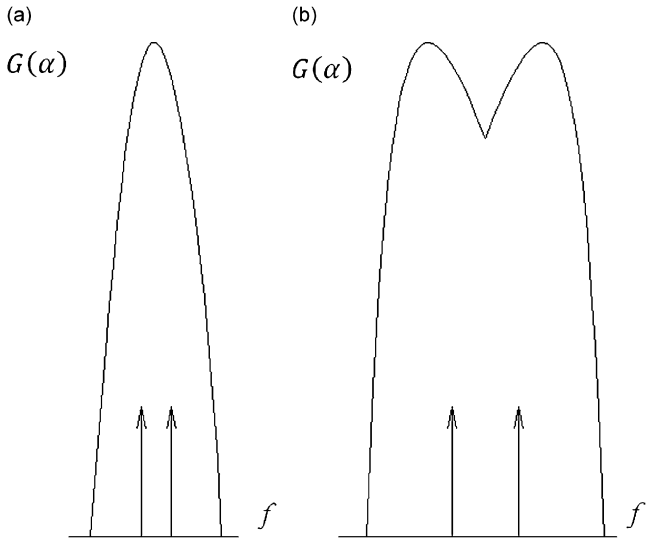

Fig. 3. Cut of the spatial frequency–temporal frequency spectrum, in which the spatial frequency axis has been converted to the incidence angle: (a) non-resolved sources due to a lack of resolution and (b) resolved sources.

Here, the integers are multiples of the fundamental distance d, in a way that the reference microphone (microphone 1) is placed at position 0 in the linear array (higher end), microphone 2 is placed *1d* under microphone 1, microphone 3 is placed *2d* under microphone 1… Under these circumstances, the array resolution can be computed for different incidence angles of the sound waves as follows:

$$\Delta\alpha = \lambda/(2L\cos\alpha)$$

The worst resolution case will be for the lowest frequency (88 Hz, see Section 2) since the wave length is the largest. Table 1 lists the antenna resolution for different incidence angles in the worst case.

The first conclusion drawn from Table 1 is that, the nearer the incidence angle is to $\pm 90^\circ$, the lower the resolution. If resolution is understood to be the minimum angular distance that must exist between two sources of the same strength in order to be separated by the antenna (Fig. 3), then Table 1 states that a source placed near $\pm 90^\circ$ will mask all the other sources.

As said in Section 3, noise coming from upper positions (from now on, positive angles) will correspond to airplane noise, and noise coming from lower positions (negative angles) will correspond to urban noise. Therefore, if traffic noise is seen under -90° (or near) its lobe basis penetrates into positive angles masking noise coming from positive angles, if present. Therefore, the placement of the antenna in sites with urban noise impinging with an incidence angle near -90° are not suitable. When the noise caused by an airplane is impinging at 90°, the spreading of the lobe is not such a problem since a pure urban noise time register is not the goal of this study, so there is no problem having it masked.

On the other hand, the resolution also gives a measure of the width of the lobe, so the lobe of a source placed at -20° will spread (half the resolution at each side) until almost 0°. Therefore, urban traffic noise impinging within -20° to 0° may invade positive angles (see Table 1). As a consequence, sites with urban traffic noise impinging within 0° and -20° should be avoided. The array has to be placed high enough in relation to the urban sources. Specific situations have to be taken into account, for instance, eventual noise generated by a distant road may reach the array with an incidence angle near 0°. However, noise level

generated on such a road may be much lower than the airplane noise in the array position, so the influence could be neglected. Moreover, not only direct noise has to be taken into account when placing the array, but also reflected urban noise, which is important as it may impinge on the array within the mentioned critical angular range.

4.1. Data acquisition

The acquisition system is based on three ADLINK PXI-2006 acquisition cards synchronized with an external timer ADLINK cPCI-8554/R.The microphones used are the comparatively low cost Behringer ECM 8000, corrected in amplitude and phase in order to ensure that all of them have the same frequency response.

In order to avoid aliasing, the signals are low pass filtered before being acquired. The cut-off frequency has been stated slightly higher than the maximum frequency of interest. As a consequence, given that this limit is 2828 Hz, the acquisition device has to be capable of sampling each channel at least at 7.5 kHz, according to Nyquist's theorem. On one hand the block size value must be a power of two in order to use fast Fourier algorithms to compute the Fourier transform of the temporally acquired data. On the other hand, a data segment with the duration of one second must be acquired to calculate $L_{eq_{1s}}$ (as sound level meters do). Therefore, the sampling frequency and the block of acquired data have both been rounded to 8192 to fulfill these two requirements.

A Hamming window with $\alpha = 0.7$ is applied in both spatial and temporal Fourier Transforms. In order to reduce the amount of data after performing the temporal transform, data has been averaged over 1/12 octave. After that, frequency resolution is still high enough in relation to angular resolution of the antenna to avoid unsharp images as a result of averaging.

Finally, after spatial transform, the data can be added over all positive angles, and over all negative angles separately, and also the addition can be made over standardized 1/1—octave. In that way $L_{eq_{1s}}$ 1/1—octave spectrum can be obtained for aircraft generated noise and for urban noise separately.

5. Results

5.1. Simulations

In this section, laboratory tests are made in order to check the resolution of the array. As mentioned before, resolution can be understood as the minimum angular distance that must exist between two sources of the same strength in order to be separated by the antenna. Therefore, to check the antenna resolution, the situation of having two sources impinging on the array, has been simulated by computing the ideal response of each microphone. In this experience the array's response has been simulated having two waves impinge on it; the first with an angle of incidence of 20° (which can be understood as an aerial source), and the second with an angle of -20° (the upper limit value for the angle of incidence of urban noise, see Section 4). Both waves have an amplitude of 70 dB and the same frequency and are assumed to be plane waves. Fig. 4 and Table 2 show the results for different wave frequencies.

In all cases the two waves are visually resolved but because the resolution is frequency dependent, it became poorer on the 125 Hz octave. If the angle range is widened between 5° and 45° and -5° and -45°, the expected noise level is obtained, and the resolution is sufficient for the objectives of this study. The last column of the table shows the sum of the energy throughout all the angles in the polar graph, which equals 73 dB, and which is within the expected range (70–76 dB) in the case of two coherent waves.

A second test has been performed; the response of every microphone when a wave-front is impinging with an incidence angle of -20° (referring to the microphone at the higher end of the array) has been simulated. Subsequently the simulated microphone's output signals have been processed as explained in Section 3.1. An incidence angle of -20° is chosen because it represents the maximum allowable angle for traffic noise. Fig. 5 shows the response of the array for different frequencies. The level of the impinging noise is 70 dB at the array.

Table 3 reveals that in order to reduce error in noise level estimation, noise has to be integrated in the whole area of negative angles (-90°, 0°), or the inverse if the source was seen in a positive angle. It is important to highlight the fact that, although no source is present on the positive angles, noise level for that range of angles

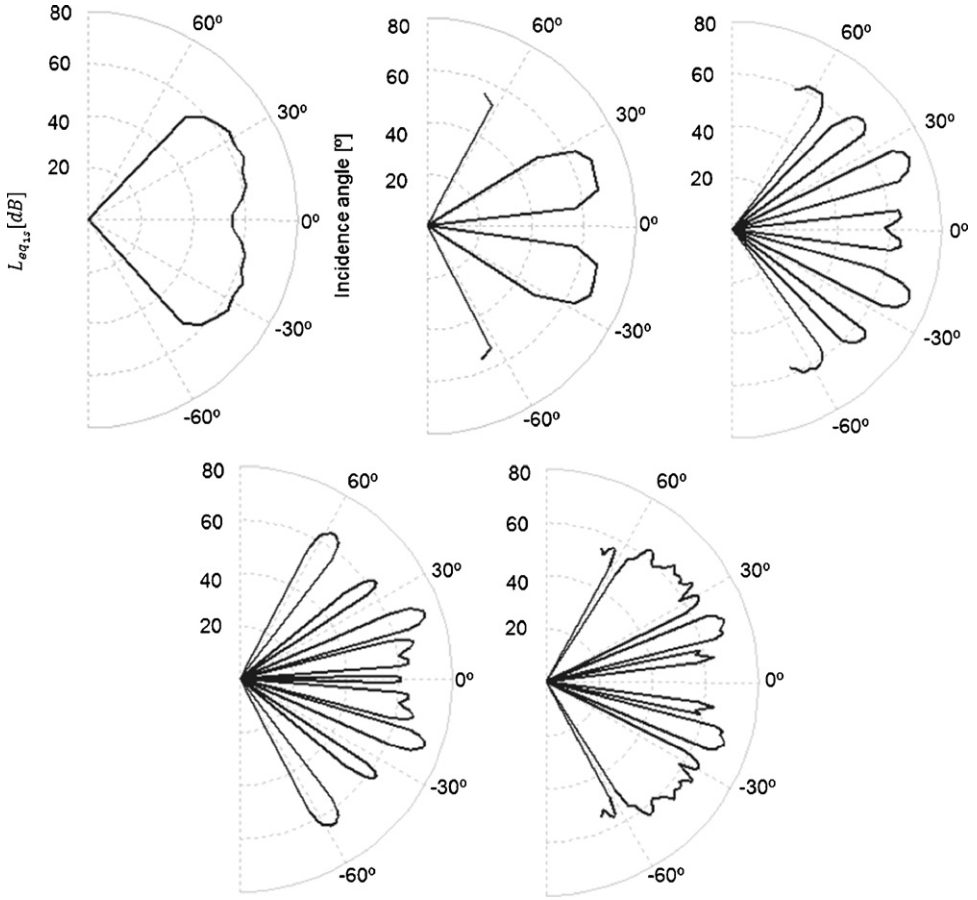

Fig. 4. Array output for two symmetrical waves of 125, 250,500, 1000, and 2000 Hz (same scale for all diagrams). The metric used is the $L_{\mathrm{eq}_{1s}}$.

Table 2
Noise level in dB integrated in different ranges of angles (columns) and different frequencies (rows) for the case of multiple sources simulation.

	−45°, −5°	−30°, −10°	−25°, −15°	15°, 25°	10°, 30°	5°, 45°	−90°, 90°
125	70	67.6	64.9	65.1	67.8	70.1	73.3
250	70.4	70.3	68.1	68.1	70.3	70.4	73.5
500	69.2	68.2	68.01	68.01	68.2	69.2	72.9
1000	69.6	69.2	68.9	68.9	69.2	69.6	73.2
2000	68.7	68.5	68.5	68.5	68.5	68.7	72.7

The reference level is of 70 dB.

is not 0, but is influenced by the presence of sources in the negative angles quadrant. If −90°, 0° column is taken as noise in negative angles and column 10°, 70° represents noise in positive angles, it is important to notice that at low frequencies noise in positive angles is 14 dB below noise in negative angles, and at high frequencies the difference reduces to 8 dB. Anyway, measured noise in positive angles is always at least 8 dB lower that the noise in negatives.

This fact will influence the antenna performance when measuring aircraft noise. Several situations can be considered:

Urban noise present and absence of aircraft noise: When the antenna is placed in its operation site, noise coming from positive angles quadrant record is influenced by the existence of noise coming from negative

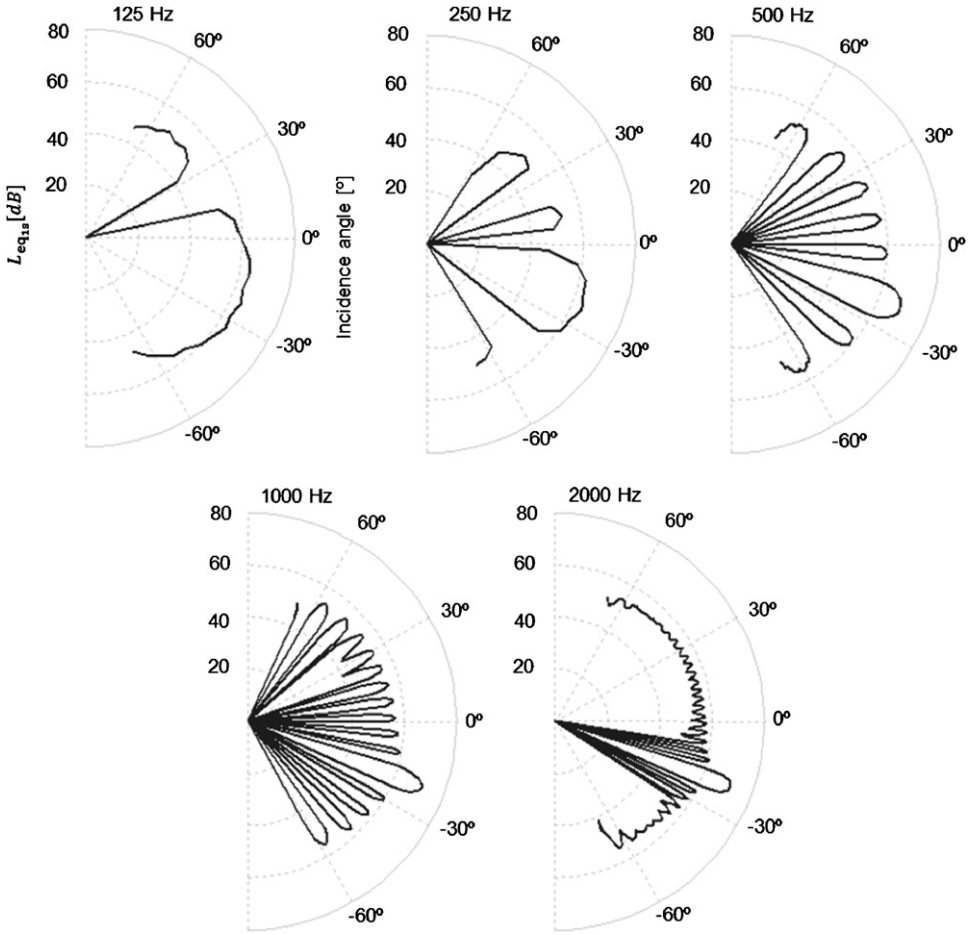

Fig. 5. Array output for a single wave impinging with −20°. The wave frequency is 125, 250, 500, 1000, and 2000 Hz (same scale for all diagrams). The metric used is the $L_{eq_{1s}}$.

Table 3
Noise level in dB integrated in different ranges of angles (columns) and different frequencies (rows) for the case of a single source simulation.

	−70°, −35°	−70°, −30°	−35°, −5°	−30°,−10°	−10°, 10°	−5°, 70°	10°, 70°	−90°, 0°
125	62.6	64.7	68.3	66.7	63.6	62.1	56.1	70.1
250	56.5	61.9	69.6	68.6	58.7	58	57.1	70.1
500	57.3	57.3	69.2	69.2	55.8	59.8	57.8	69.9
1000	58.7	58.7	69	69	54.7	61	59.9	69.9
2000	58.9	60.1	68.7	68.4	59.4	63.5	62.3	70.2

The reference level is of 70 dB.

angles quadrant. This is because in the presence of urban noise and the absence of airplane noise, not only the main lobe which points in the direction of arrival of urban noise appears, but also a set of secondary lobes (see Figs. 4 and 5). These secondary lobes may extend to positive angles causing the noise on the airplane time history to be different from 0. These secondary lobes are proportional to the main lobe, so the airplane noise record is proportional to the urban noise record but with a lower level. In other words, both records are parallel.

Aircraft noise predominates over urban noise: When an airplane is flying over the array, the urban noise record will rise for the same reason given above if the airplane noise level is significant with regard to the urban noise. What will happen in all cases is that both records will not remain parallel during the fly-over, because the noise growth in positive angles will be greater than the growth in negative angles. This fact has been used here as a trigger to distinguish the peaks generated by an airplane fly-over. When the difference between urban noise and aircraft noise reduces below a certain threshold value, the noise in the positive angles record is ascribed to the aircraft. Whenever this condition is not fulfilled, aircraft noise is presumed to be 0.

Aircraft and urban noise events contributions are similar: In such a case, both positive and negative angles noise record will raise a similar amount, and also will influence each other by a similar amount. As the noise measured over the positive angles quadrant ($L_{eq}^{\alpha>0}$) will be almost the same that the noise measured over the negative ($L_{eq}^{\alpha<0}$), the difference between them will be under the threshold value, and consequently the noise in the positive quadrant will be assigned to the aircraft. However, the influence of the noise in the negative quadrant needs to be analyzed. Taking the previous idea that the contribution caused by urban noise side lobes in the positive angles quadrant is as much $L_{eq}^{\alpha<0}-8$ dB, the sound measured over the positive angles quadrant will be:

$$L_{eq}^{\alpha>0} = 10\,lg(10^{L_{eq}^{airplane}/10} + 10^{L_{eq}^{\alpha<0}-8/10})$$

Then, assuming that both sources have a similar emission in the array, the sound assigned to the airplane ($L_{eq}^{\alpha>0}$ will be 0.6 dB higher than the real noise level of the airplane ($L_{eq}^{airplane}$). In conclusion, the influence of the urban noise in the airplane noise measurement is negligible even if the source emission of both sources in the array is similar.

Aircraft noise reflections on the floor impinge on the array: This situation is similar to the previous one since reflections would cause, in the negative quadrant, a similar noise level than the one generated by the direct noise in the positive quadrant. Therefore, if a proper placement of the array cannot be found in terms of avoiding noise floor reflections on the array (it is mandatory to avoid reflections in other building facades), the noise level assigned to the airplane will be as much 0.6 dB higher than the real one.

Absence of aircraft noise and urban noise: If the array were placed in a site with low urban noise, the trigger condition would fail because, if neither airplane nor urban noise is present, no difference would exist between either registers, so the software would consider that airplanes are flying over constantly. In order to avoid this, a second condition is set for the trigger to be valid; airplane noise time history should be over 35 dBA in order to accept that a plane is passing overhead.

5.2. Tests inside the semi-anechoic chamber

The aim of this section is to check the real performance of the antenna in comparison to the results obtained in the simulation. In order to reduce the effect of extraneous factors, this test was carried out in a semi-anechoic chamber. Due to the limited dimensions of the chamber, the test was performed at a factor scale of 1:2.

An experiment was designed emulating practical conditions in a very simplified way. A loudspeaker fed with pink noise was fixed at -20° from the array representing an urban noise source placed at the highest incidence angle allowed for these sources. Also mobile sound sources (representing aircraft noise) were placed

Table 4
Antenna output level for two simultaneous sources at different angular distances.

Static source at -20°		Mobile source		
Expected level (dBA)	Array level (dBA)	Angle (°)	Expected level (dBA)	Array level (dBA)
70	71.4	5	69	65.5
70	70.4	25	69	68.8
70	70.5	45	69	69
70	70.5	60	69	69.3

alternatively in different positions, keeping a constant distance with the array and therefore having, in all cases, the same emission level on the array.

Both sources have a very similar strength (see Table 4), but for the case when the mobile source is closer to the source placed at -20°, although they are visually resolved (Fig. 6a), neither their strength nor their incidence angle can be evaluated correctly. This is not a problem because hopefully hardly any aircraft with a noticeable sound contribution will be seen at 0° by the array if it is placed in urban environment. In all other cases (Fig. 6b–d) both sources are resolved and its contribution is correctly calculated (see Table 4).

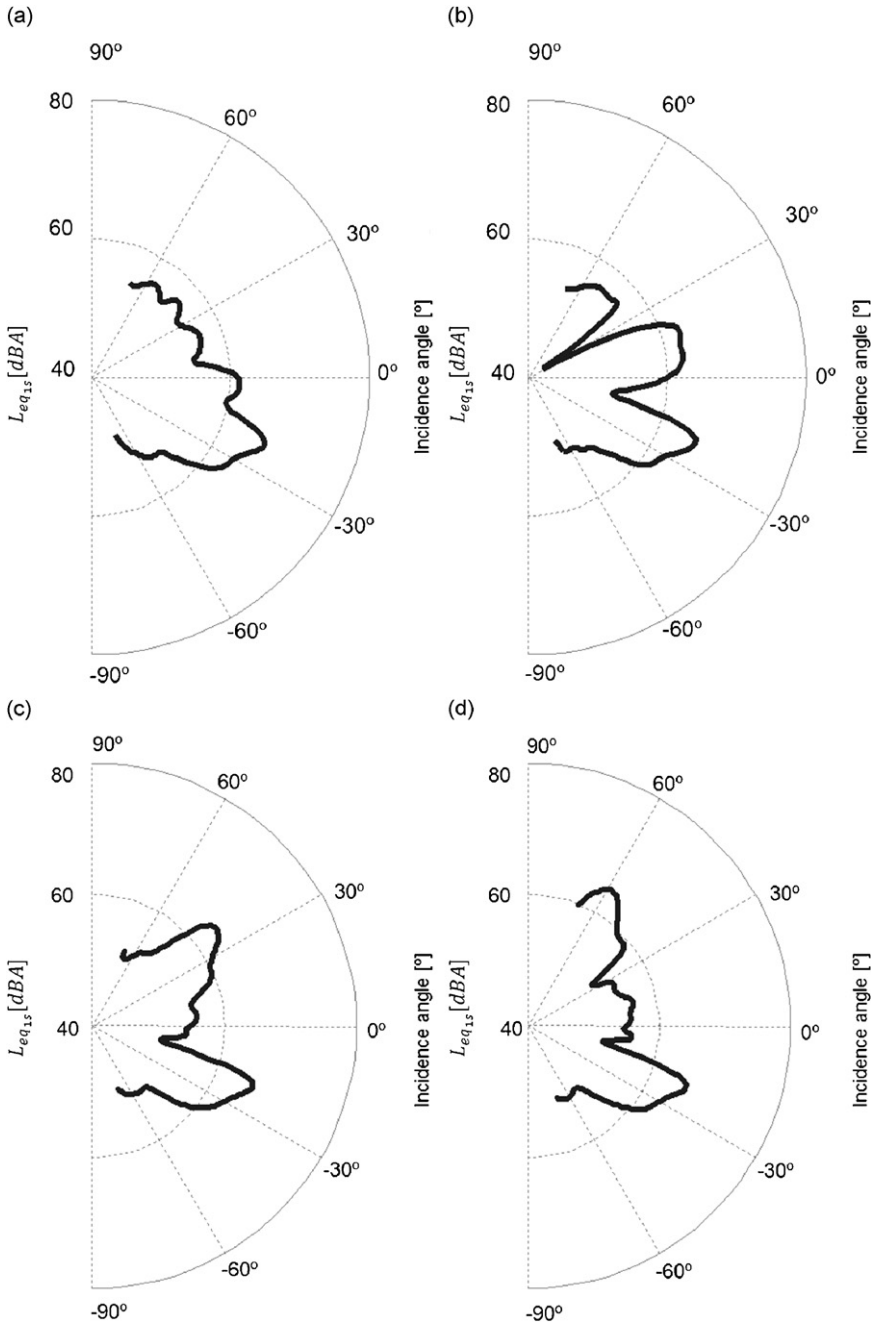

Fig. 6. Noise level (averaged $L_{eq_{1s}}$) measured by the array when there is a source at -20° and another source at: (a) 5°, (b) 25°, (c) 45°, and (d) 60°.

Fig. 7. Experimental setup for outdoor tests, the array was placed at the edge of a terrace high enough with respect to the street and the surrounding buildings to ensure that no urban noise was impinging within the critical angular incidence range. At the top of the array it can be seen the outdoor microphone of the sound level meter.

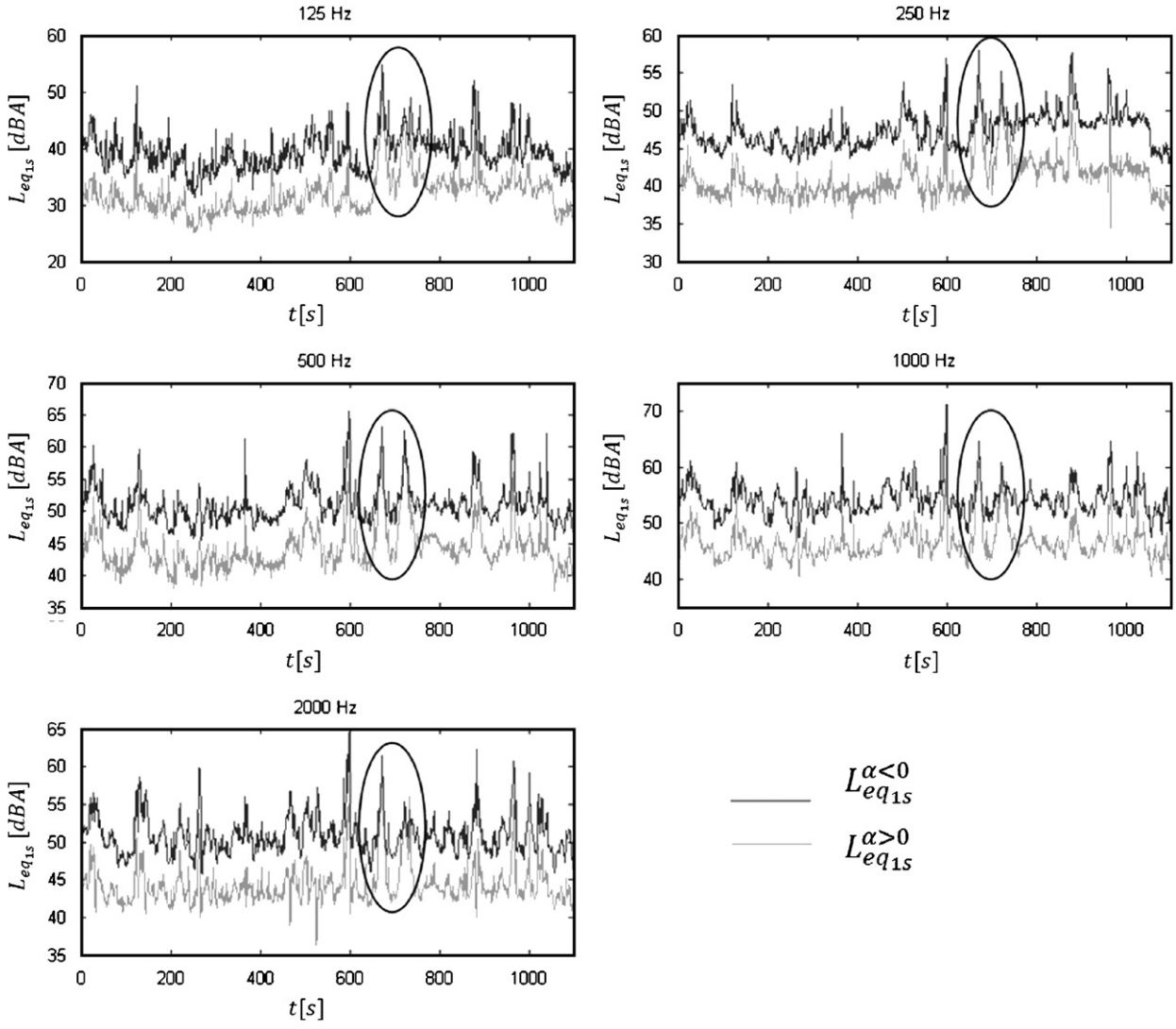

Fig. 8. $L_{eq_{1s}}$ time history for noise coming from negative angles and from positive angles. The results are showed separately for every octave band, and airplanes fly-over are circled.

In Table 4 expected strength values for each source (measured with a sound level meter) can be compared with the array's estimation (called "array level" in the table). The latter value is obtained by integrating the sound pressure level for a range of 25° around the main lobe's maximum. As mentioned before, only in the case where the mobile source is at 5° is the estimation not correct (see Fig. 7).

5.3. Outdoor tests in airport surroundings

The antenna is placed on the roof of a five-floor building; which is overflown mostly by light aircraft; the emission levels of which are not high enough to promote an environmental impact study. Therefore, the antenna is tested in more demanding conditions than their normal operating conditions since light aircraft noise and urban traffic noise levels are similar. The placement ensures that urban traffic noise impinges on the array under −20°.

Simultaneously to the measurement, attention was paid to the different noise sources causing the sound field. For instance, note was taken of the time when an airplane was passing by, a noisy motorcycle passed, an

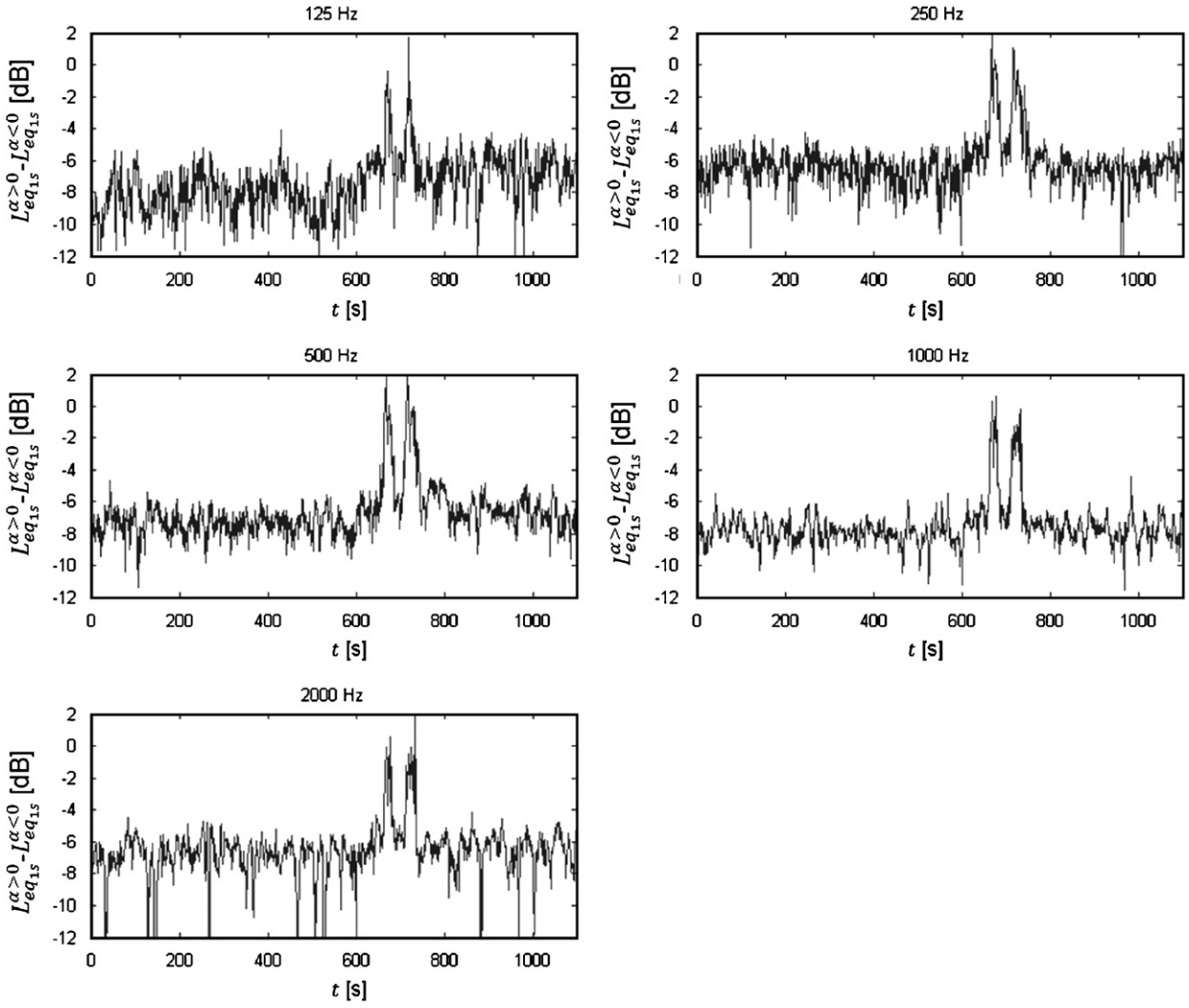

Fig. 9. Time history for the difference of $L_{eq_{1s}}$ between the noise history for positive angles and the noise history for negative angles. The results are shown separately for every octave band; the sharp peaks in the register correspond to aircraft noise events.

automobile sounded the horn and so on. This was done to make it easy to recognize the factors that generate every single peak in the noise record.

Fig. 8 depicts the $L_{eq_{1s}}$ time history for noise in negative and positive angles. The record is for a 20 min period of measurement. During this period two light aircraft flew over the antenna, the first one passed within $t = 654$ and 687 s, and the second one within $t = 706$ and 752 s. As stated when explaining the processing algorithm, after decomposing the sound field in the direction of its component waves, two different $L_{eq_{1s}}$ records are obtained. The first one integrates all sound energy coming from negative angles, which is associated with urban noise sources, and the second one contains the energy from positive angles, which refers to aerial sources.

Not one of these records is a pure record of urban noise or aerial noise because the record of noise coming from positive angles also includes the contribution of the sidelobes created by sources placed on negative angles (Section 5.1), and the record of noise coming from negative angles includes aircraft noise reflections, which impinges on the array with a negative angle. Therefore, when there is no airplane flying over the array, the record of the noise coming from positive angles is at least 4 dB under the record of the noise coming from negative angles because of the sidelobes (Section 5.1), and when there is an airplane flying over the array the

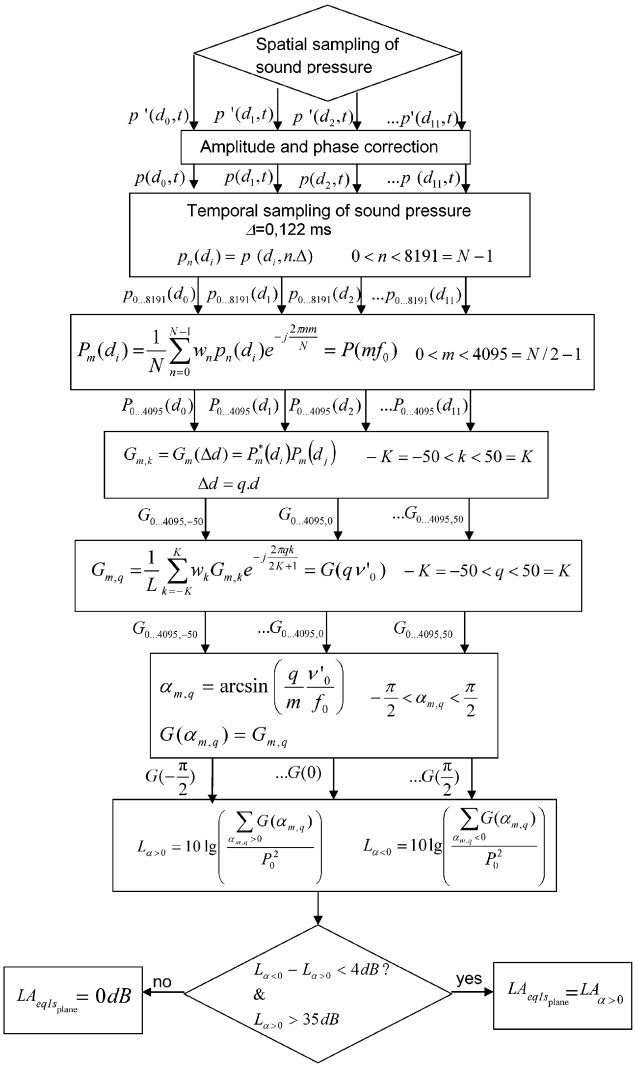

Fig. 10. Block diagram showing the different steps of the processing algorithm, the order they are performed, and the intermediate data obtained (near the arrows).

two records became closer. In Fig. 8 airplane generated peaks are circled, and it can be seen that the gray and black lines approach each other, while for the rest of the record they keep their distance.

The results show that, when no airplane noise is present, airplane noise time history has the same shape as urban noise time history but between 4 and 11 dBA lower. The reason for this effect has been explained in Section 5.1.

To make this clearer, Fig. 9 shows the difference between an aerial noise and an urban noise record. It can be seen that the peaks in this record coincide in time with the flying over of the airplanes, while for other instants the record is not sharp.

When the difference between the two records reaches −4 dB value it acts as a trigger to obtain a pure aircraft noise record. From this moment until the difference goes under −4 dB, $L_{\mathrm{eq}_{1s}}$ measurements of the record of noise coming from positive angles are accepted as a pure aircraft noise recording. For all other cases pure aircraft noise recording still provides 0 dB.

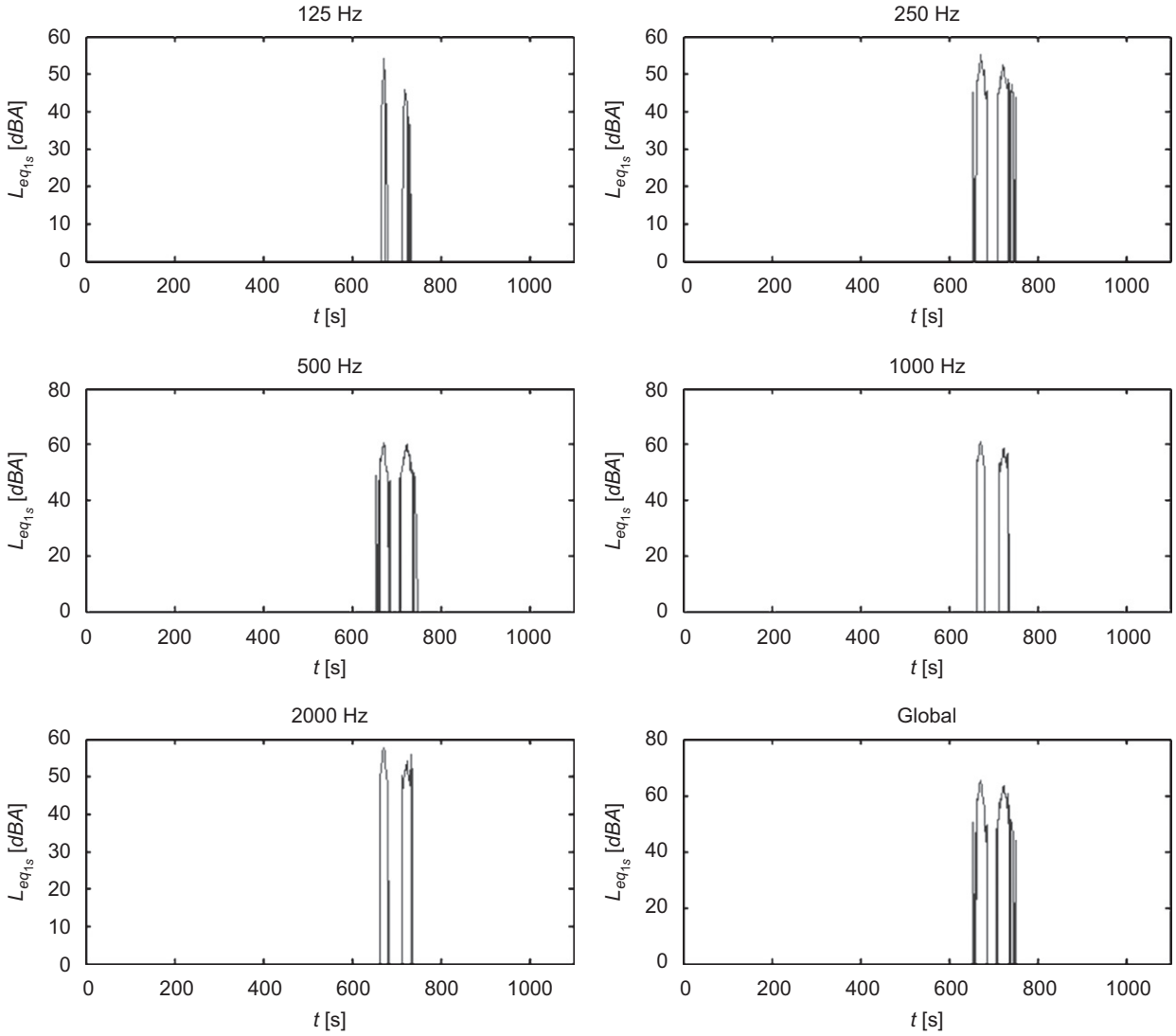

Fig. 11. Final $L_{\mathrm{eq}_{1s}}$ noise history provided by the antenna, only noise events due to aircraft fly-over remains while at any other time 0 dBA is provided. The results are shown separately for every octave band.

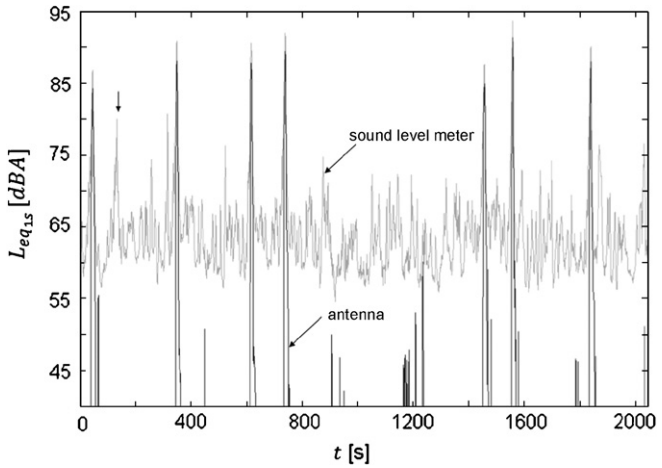

Fig. 12. Comparison between antenna's result and the sound level meter measurement. The metric used is overall $L_{eq_{1s}}$.

The processing algorithm including the trigger conditions that have to be fulfilled in order to consider that an airplane is flying over, i.e. 4 dB between both registers and 35 dB of aircraft noise, is summarized in Fig. 10. The threshold values for the two conditions can be adapted to new antenna placements.

Fig. 11 shows this final pure aircraft noise recording for the measurement period treated in this section. Such a record is the final result of the array and it is provided on-line when the device is running.

Fig. 12 shows the final result given by the array, and also the signal recorded simultaneously by a sound level meter. From Fig. 12 it can be seen that the array provides a record where all noise not generated by airplanes has been removed. The arrow points towards a peak which is not due to an aircraft passing, and does not appear in the array record. This is an example of how the array result is not influenced by noise different from that caused by airplanes.

6. Conclusions

This paper proves that a linear sparse microphone array of 12 elements and 3 m long can be used to obtain an aircraft noise time history not influenced by extraneous noise such as traffic noise or other sorts of urban noise. This device can be used in a wide range of urban placements only requiring care to be taken to avoid urban noise impinging within 0° and -20°, and airplane noise impinging near 90°.

The different tests have revealed a good performance of the array in the frequency range between 125 and 2000 Hz octave bands. In spite of this, the resolution of the device is not high enough to provide a clean aircraft noise record by only applying frequency domain beamforming to the spatial cross-correlations of the microphones'signals. The problem appears when no airplane is flying over, the antenna output should be 0 but is not because of the effect of the traffic noise secondary lobes. Therefore, a new step to the processing algorithm has been added to identify the exact time period of over-flying. This step consists of comparing the aerial noise time history and the urban noise time history obtained from applying frequency domain beamforming to the spatial cross-correlations, and taking as a trigger the moment when both curves stop going parallel. From this instant until parallelism is restored, aerial noise register is ascribed to airplane noise, and for all other time instants aerial noise is 0.

Acknowledgment

This work was funded by Boeing Research & Technology Europe S.L.

References

[1] R. Rylander, M. Björkman, Annoyance by aircraft noise around small airports, *Journal of Sound and Vibration* 205 (1997) 533–537.

[2] C.P. Stollery, G. Rasmussen, What use can be made of the recent technological advances in outdoor instrumentation, *Proceedings of the 1994 International Congress on Noise Control Engineering*, Vol. 1, Institute of Noise Control Engineering, Yokohama, Japan, 1994, p. 217.

[3] S. Yotov, Sustantive features of Sofia airport noise monitoring system, *InterNoise*, In97-194, Budapest, Hungary, 1997.

[4] R.C. Muchall, Experiences with an intelligent measurement system for monitoring aircraft noise without radar assistance, *InterNoise*, The Hague, Holland, 2001, p. 2019.

[5] K.M. Adams, Aircraft noise event detection—the threshold problem, *InterNoise*, Prague, Czech Republic, 2004, p. 182.

[6] O.-H. Bjor, J.E. Bjørn Winsvold, Sound intensity for identification of aircraft noise, *InterNoise*, The Hague, Holland, p. 1959.

[7] W. Wszolek, R. Tadeusiewicz, Evaluation of usefulness of artificial intelligence methods in aviation noise monitoring systems, *Proceedings of the 10th International Congress on Sound and Vibration ICSV10*, Stockholm, Sweden, pp. 709–716.

[8] R. Tadeusiewicza, W. Wszolek, A. Izworskia, T. Wszolek Utilization of artificial intelligence methods for assistance in interpretation of acoustic signals, *European Conference on Noise Control*, Naples, Italy, 2003.

[9] K.M. Adams, B. Esler, Advances in acoustic recognition of aircraft noise events, *InterNoise*, Newport Beach, CA, USA, 1995, p. 1129.

[10] K.M. Adams, Aircraft noise evaluation-A comparison between conventional event detection and neural network classification, *InterNoise*, Port Lauderdale, FL, USA, 1999, p. 1043.

[11] K.M. Adams, Success and failure analysis of neural network identification of aircraft noise, *InterNoise*, The Hague, Holland, 2001, p. 2221.

[12] H. Sakai, S. Sato, N. Prodi, R. Pompoli, Measurement of regional environmental noise by use of a PC-based system. An application to the noise near airport "G. Marconi" in Bologna,, *Journal of Sound and Vibration* 241 (2001) 57–68.

[13] M. Genescà, J. Romeu, M.M. Boone. Design and test of an 8-microphone array for sound sources location, *XXXIII Congreso Nacional de acústica—EAA Symposium on Urban Acoustics*, 2003-AAM-053, Bilbao, Spain (in Spanish).

[14] H. Johnson Don, D.E. Dudgeon, Array signal processing—concepts and techniques, in: A.V. Oppenheim (Ed.), *Signal Processing Series*, Prentice-Hall, Englewood Cliffs, NJ, 1993.

[15] R. Boone, Design and development of a synthetic acoustic antenna for highly directional sound measurements, PhD Thesis, TU Delft, Delft, 1987.

[16] J.D. Van Der Toorn, H. Hendriks, T.C. Van Den Dool, Measuring TGV source strength with Syntacan, *Journal of Sound and Vibration* 193 (1) (1996) 113.

[17] B. Barsikow, Experiences with various configurations of microphone arrays used to locate sound sources on railway trains operated by the DB AG, *Journal of Sound and Vibration* 193 (1) (1996) 283–293.

[18] M. Genescà, J. Solé, J. Romeu, G. Alarcón Pantograph noise measurements in Madrid–Sevilla high speed train (AVE), *InterNoise*, Prague, Czech Republic, 2004, p. 293.

[19] B. Barsikow, et al., Wheel/rail noise generated by a high-speed train investigated with a line array of microphones, *Journal of Sound and Vibration* 118 (1) (1987) 99–122.

[20] M.A. Pallas, J. Lelong, Investigation of the rolling noise sources on the tram of Nantes with a microphone array, *InterNoise*, The Hague, Holland, 2001, p. 2127.

[21] U. Michel, et al., Localisation of sound sources on moving vehicles with microphone arrays, *InterNoise*, Prague, Czech Republic, 2004, p. 782.

[22] T.C. Van Den Dool, M.M. Boone, Microphone T-array technology for moving noise source measurement, *InterNoise*, Nice, France, 2000.

[23] S. Putcrabey, P. Bertrand, A. Jacques, Localization of flow noise sources on high speed train models in anechoic wind-tunnel, *InterNoise*, IN94-181, Yokohama, Japan, 1994.

[24] G. Hölzl, et al., Deufrako. 2. Localized sound sources on the high-speed vehicles ICE, TGV-A, and Transrapid 07, *InterNoise*, In94-193, Yokohama, Japan, 1994.

[25] J.F. Hamet, M.A. Pallas, K.P.S. Deufrako, 1. Microphone array techniques used to locate acoustic sources on ICE, TGV-A and Transrapid 07, *InterNoise*, Yokohama, Japan, 1994, p. 187.

[26] M.A. Pallas, The focussed vertical array for the description of the noise sources on a moving car, *InterNoise*, Nice, France, 2000.

[27] A. Mast, et al., Harmonoise WP 1.1-Source characterisation of moving vehicles with 'acoustic camera' antenna technique, *Euronoise*, Naples, Italy, 2003, p. 268.

[28] G.P. Howell, A.J. Bradley, M.A. McCormick, J.D. Brown, De-Dopplerization and acoustic imaging of aircraft flyover noise measurements, *Journal of Sound and Vibration* 105 (1) (1986) 151–167.

[29] M. Mosher, Phased arrays for aeroacoustic testing: theoretical development, *AIAA/CEAS Aeroacoustics Conference,* AIAA 96-1713, State College, PA, 1996.

[30] P. Sijtsma, H. Holthusen, Source location by phased array measurements in closed wind tunnel test sections, *AIAA/CEAS Aeroacoustics Conference and Exhibition*, AIAA-99-1814, Bellevue, WA, 1999.

[31] R. Stoker, R. Shen, An experimental investigation of airframe noise using a model-scale Boeing 777, *AIAA Aerospace Sciences Meeting and Exhibition*, AIAA 2001-0987, Reno, NV, 2001.

[32] R. Stoker, J. Underbrink, G. Neubert, Investigation of airframe noise in pressurized wind tunnels, *AIAA/CEAS Aeroacoustics Conference and Exhibition*, AIAA/CEAS 2001-2107, Maastricht, Netherlands, 2001.
[33] U. Michel, et al., Flyover noise measurements on landing aircraft with a microphone array (Boeing), *AIAA/CEAS Aeroacoustics Conference*, AIAA 98-2336, Toulouse, France, 1998.
[34] J.F. Piet, G. Elias, P. Lebigot, Localization of acoustic source from a landing aircraft with a microphone array, *AIAA/CEAS Aeroacoustics Conference and Exhibition*, AIAA-99-1811, Bellevue, WA, 1999.
[35] G. Nishinomiya, F. Suzuki, F. Sasaki, Aircraft noise identification system by correlation technique, *Transactions on Broadcasting* 2 (1979) 697.
[36] K. Fukushima, Discrimination of aircraft noise using sound arrival direction for unattended noise monitoring system, *InterNoise*, 2003-N814, Korea.
[37] A. Mast, M.M. Boone, T.C. Van den Dool, An experimental microphone antenna array for measuring aircraft noise, *InterNoise*, The Hague, Holland, 2001, p. 2115.
[38] G.L Oh, C.L. Yap, S.K. Pang, Sound localization in the atmosphere using a big sensor array, *InterNoise*, The Hague, Holland, 2001, p. 2049.
[39] F.A. Farrelly, et al., Acoustic event localization by means of passive transducer arrays in environmental monitoring, *Euronoise*, Naples, Italy, 2003, p. 517.
[40] M.M. Boone, Model based prediction of aircraft noise parameters from pass-by noise measurements, *InterNoise*, 2002-N300, Dearborn, MI, USA.
[41] M.M. Boone, et al., Microphone array technology for aircraft noise measurements, *InterNoise*, Nice, France, 2000, pp. 28–30.
[42] ISO 9613-1:1993 Attenuation of sound during propagation outdoors—part1: calculation of the absortion of sound by the atmosphere, 1993.
[43] D.A. Linebarger, Difference bases and sparse sensor arrays, *IEE Transactions on Information Theory* 39 (2) 1993.